International Journal of Thin Films Science and Technology

http://dx.doi.org/10.18576/ijtfst//130308

Investigation on copper doped CdTe thick films for optoelectronic applications: structural, optical and electrical characteristics

Khairiah Alshehri

Department of Physics, College of Science, University of Bisha, Bisha 61922, Saudi Arabia

Received: 18 May 2024, Revised: 22 Aug. 2024, Accepted: 25 Aug. 2024
Published online: 1 Sep. 2024

Abstract: This study focuses on the effects of replacement Cd with Cu on the structural, optical, and electrical properties of CdTe one micron thin film. In this regard, CdTe ingots with Cu concentrations from 0 to 10 at.% were produced via mechanical ball milling at 200 rpm for 6 hours, then shaped into disks for thin film deposition. Films with a 1000 nm thickness were deposited onto glass substrates by electron beam at room temperature, after cleaning and evacuating the chamber to 510^{-6} Pa. XRD and EDXS analyses confirmed Cu incorporation and retention of the cubic structure. In terms of spectral ellipsomeric, three optical layer models (adhesive layer of the substrate/B-spline layer of CdTe:Cu film/surface roughness layer) are used to determine the thickness of the film with high accuracy. Optical measurements showed that increasing Cu content led to larger crystallite sizes, reduced micro-strain, and a blue shift in the absorption edge, indicating a wider band gap. Refractive index and extinction coefficient calculations revealed a decrease in refractive index with higher Cu doping, suggesting improved transparency and favorable band gap characteristics for photovoltaic applications. Electrical measurements using the four-point probe method showed that increasing Cu content from 0 to 10 at.% decreased sheet resistance from 49.9 Ω to 1.65 Ω and increased conductivity from 200 $(\Omega.cm)^{-1}$ to 6000 $(\Omega.cm)^{-1}$. Carrier concentration and Hall mobility were also improved, suggesting that CdTe films with 10 at.% Cu are optimal for high-efficiency CdTe solar cells.

Keywords: 1-micron CdTe:Cu films; Microstructural properties; Optical properties; optoelectronic applications.

1 Introduction

Cadmium telluride (CdTe) is a semiconductor material with a wide range of applications, particularly in photovoltaic devices, radiation detectors, and optoelectronic devices due to its direct bandgap (1.5 eV at room temperature) and high absorption coefficient $(alpha \approx 10^5 cm)^{-1}$ [1]. The properties of CdTe can be significantly influenced by doping, which introduces additional elements into the semiconductor to modify its electronic structure and enhance performance. Among various dopants, copper (Cu) has garnered interest due to its potential to improve the electronic and optical characteristics of CdTe [2].

Additionally, CdTe boasts excellent transport properties, a high average atomic number (50), substantial resistivity, and both n-type and p-type conductivity. These characteristics qualify the production of both heterojunction and homojunction solar cells [3]. Its strong absorption edge permits CdTe to absorb 90% of incident photons within a 2 mm thick layer, whereas silicon requires a 20 mm layer to achieve similar absorption [4]. These attributes make CdTe a promising material for diverse applications, including photovoltaic conversion, solar cell structures, field-effect transistors, and X-ray and gamma-ray detectors [5,6].

CdTe thin films have been manufactured using various deposition methods, such as RF sputtering [7], chemical bath deposition [8], pulsed laser deposition [9], close-range sublimation [10], electroposition [11], thermal evaporation [12], and electron beam evaporation [13]. However, achieving stoichiometric CdTe films remains challenging. This is crucial for optimizing the absorber layer in solar cell structures, as defects and impurities introduced during the deposition process can negatively impact the optoelectronic properties of the films, thereby reducing solar cell efficiency [14,15,16,17]. It has been detected that doping CdTe thin films with specific dopants (such as Co, Bi, Ag, In, Mo, and Cu) can alter their electrical and optical properties, enhancing solar cell efficiency [18,19].

* Corresponding author e-mail: kalghem@ub.edu.sa

Copper doping in CdTe has been studied for its effects on the material's structural, optical, and electrical properties. Structural modifications often manifest as changes in lattice parameters, crystal quality, and the formation of secondary phases [20]. These alterations can impact the material's performance in devices. For example, Cu-doped CdTe films have shown variations in grain size and crystallinity, which are crucial for applications requiring precise material properties [21].

Optically, Cu-doped CdTe films exhibit altered bandgap energies and optical absorption characteristics. The introduction of copper can induce additional energy levels within the bandgap, affecting the absorption spectrum and photoluminescence properties [22]. This can be advantageous for certain applications where tuning of optical properties is required, such as in sensors and imaging devices. Electrically, the incorporation of Cu can modify carrier concentration and mobility, thereby influencing the semiconductor's conductivity and overall electronic performance.

The behavior of Cu-doped CdTe in terms of charge carrier dynamics and electrical conductivity is a key area of investigation, with implications for improving device efficiency [23]. Markedly, copper (Cu) acts as an amphoteric dopant in the CdTe lattice. It can inhabit interstitial sites as Cui+, creating a shallow donor level, or substitute Cd atoms to form a deeper acceptor level as CuCd-. Additionally, Cu can form complexes with Cd vacancies (Cui++VCd-2) and Cu+-CuCd, resulting in shallow acceptors [24]. A key benefit of Cu doping in CdTe is the enhancement in carrier concentration, which can lead to better ohmic contact. The objectives of the current study are as follows: First, to investigate how varying copper (Cu) content affects the microstructural parameters (such as crystallite size and lattice strain) and optical properties of CdTe thick films. Second, to precisely measure the film thickness using spectroscopic ellipsometry. Third, to employ the Van der Pauw method along with a Hall-Effect measurement system for analysis. Finally, to evaluate the optical and electrical properties to determine the most suitable film for the absorber layer in solar cell applications.

2 Experimental Procedures

CdTe:Cu ingots with different Cu concentrations (0, 2, 4, 6, 8, and 10 at.%) were produced using mechanical milling. Analytical-grade, stoichiometric CdTe and Cu_2Te powders (both with a chemical purity of 99.999% from Aldrich) were combined and milled in a ball mill at 200 rpm for 6 hours. To prevent powder splashing during the evaporation process, the mixture was compacted into disk shapes. These pure and Cu-doped CdTe ingots were then used as sources for thin film deposition. CdTe and Cu-doped CdTe thin films with variable Cu concentrations were deposited onto amorphous glass substrates via an electron beam evaporation system (Edward Auto 306) at room temperature. The substrates and ingots were loaded into the chamber, which was then evacuated to a pressure of 5×10^{-6}Pa.

The pellet ingot was heated for 5 minutes prior to evaporation to remove contaminants and degas the material. The film thickness was controlled to 1000 nm at a deposition rate of 2 nm/sec using a thickness monitoring device (model FTM6).

Additional details about the deposition process can be found elsewhere [25]. Crystallographic analysis was conducted using an X-ray diffractometer (XRD, $Cu - K\alpha = 1.54056\mathring{A}$, Philips diffraction 1710). The elemental composition of the film was analyzed with energy dispersive X-ray spectroscopy (EDXS). Transmission and reflection spectra were recorded with a dual-beam spectrophotometer (UV-VIS-NIR, Shimadzu model). The electrical properties of CdTe:Cu films were measured by Van der Pauw method with a Hall effect measurement method (HMS-5000, ECOPIA). Resistivity, mobility, carrier type and carrier concentration are obtained on a 1 cm2 glass substrate

3 Results and discussion

3.1 Elemental, structural and microstructure characterizations

The elemental analysis of the tested thin films is carried out using the energy-dispersive X-ray spectroscopy (EDXs) microanalysis technique, which is related to electron microscopy because it generates distinctive X-rays that reveal the presence of components in the specimen.

Figure 1a shows the elemental composition analysis of CdTe:Cu (2 at.%) thin film using the EDXS microanalysis technique, while Fig. 1b exhibits that of CdTe:Cu (10 at.%) thin film. The charts for both samples reveal three distinct peaks corresponding to Cd, Te, and Cu. Additionally, the spectra indicate that as Cu doping increases, the intensity of the Cu peak also rises. This suggests that the film maintains stoichiometry and confirms the successful incorporation of Cu ions into the CdTe matrix. The X-ray diffraction (XRD), a nondestructive technique, was employed to provide detailed insights into the crystallographic structure of the thin films under study.

Figure 2a illustrates the XRD patterns for both Cu-free and Cu-doped CdTe thin films, which were produced by electron beam evaporation at ambient temperature on a glass substrate, with Cu concentrations varying from 2% to 10%.

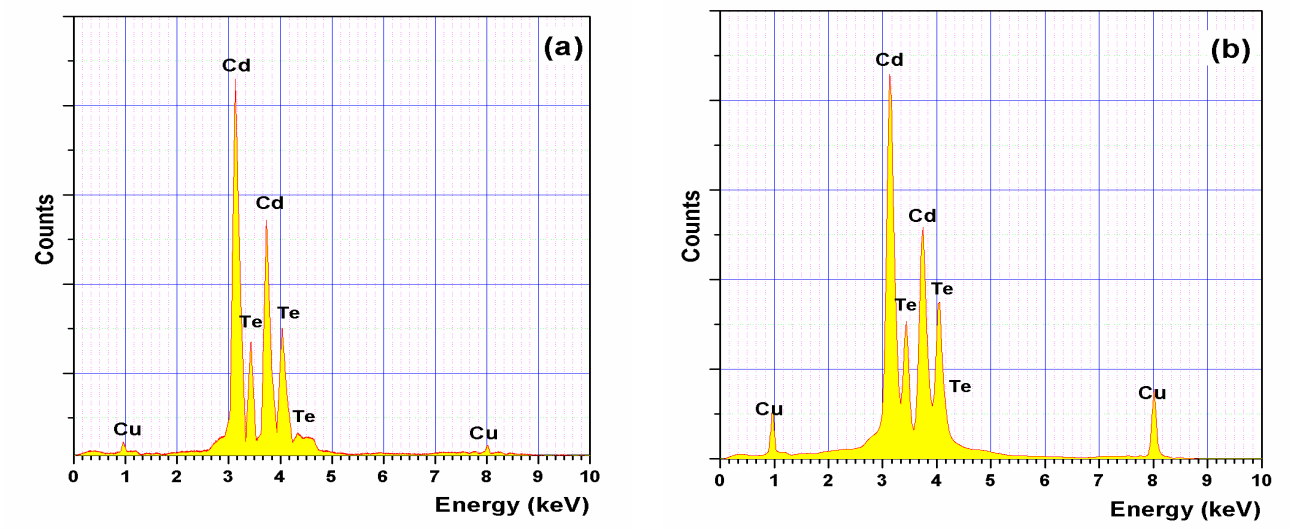

Fig. 1: EDXS spectra of (a) CdTe:Cu (2 at.%) and (b) CdTe:Cu (10 at.%) thin films.

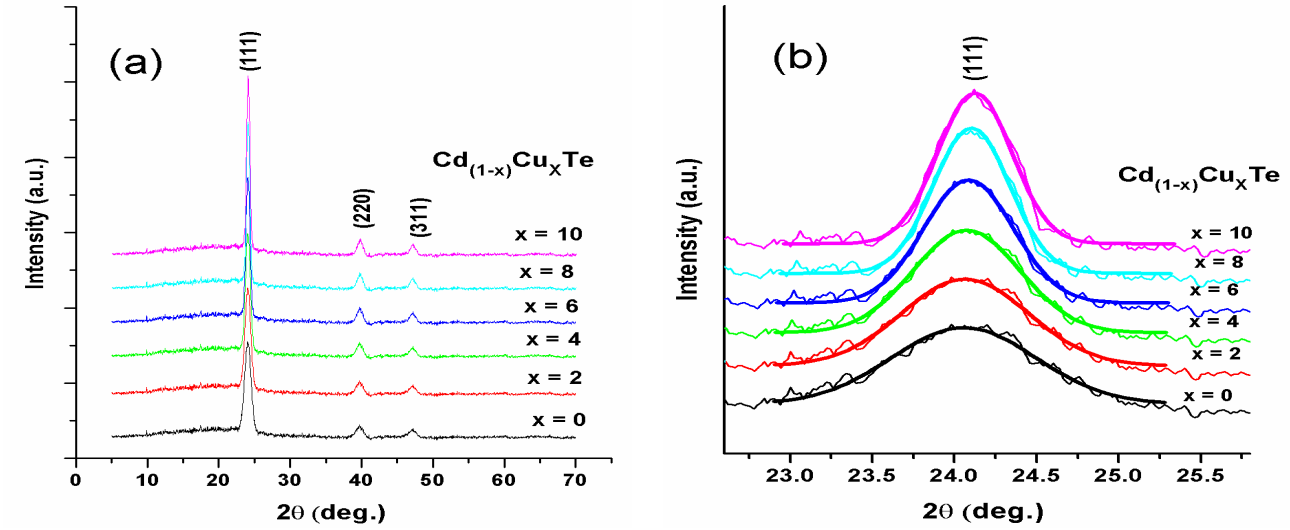

Fig. 2: EDXS spectra of (a) CdTe:Cu films and (b) The magnification of diffraction peak at (111) plane.

The patterns reveal that all films exhibit a polycrystalline-like structure, with reflection lines corresponding to the (111), (220), and (311) diffraction planes of the cubic zinc blende structure. This indicates the presence of the cubic phase of CdTe, as specified in JCPDS No. 01-075-2086. By comparing the intensities of the three phases, it can be realized that phase (111) is the dominant one, while the other phases (220) and (311) have intensities within the background of the device (measurement errors), so they can be inconsequential.

Furthermore, the XRD patterns in Figure 2a show a preference for grain development in the direction of the (111) plane owing to the energy encounter between surface and strain energy [26]. It's important to highlight that the XRD spectra showed no additional peaks related to copper phases like copper oxide or copper clusters. This indicates that Cu2+ ions were effectively incorporated into the CdTe lattice without altering its cubic structure. For more accuracy and analysis, all XRD data has been normalized to eliminate any instrumental errors that may arise during the measurement procedure.

Figure 2b shows the dominating phase/plane (111) of the normalized XRD patterns for the representative samples $x = 0wt.\%$ and $x = 10wt.\%$. The diffraction angle remains unchanged, but the peak intensity and width are reduced. This

may indicate the uniformity of composition in all thin films (same lattice parameter), as well as a decrease in internal strain owing to the inclusion of Cu ions into the CdTe structure. The Debye–Scherrer equation is widely used to estimate the average crystallite size in polycrystalline materials using X-ray diffraction data. This equation relates the crystallite size (D) and lattice strain (e) to the X-ray wavelength (λ), the diffraction angle (θ or Bragg's angle), and the full width at half-maximum (β) of the diffraction peak [24,25,26,27]. The Eq. 1, where β represents the broadening of the diffraction peak, which is the difference between the width of the observed peak (β_{obs}) and the standard peak width (β_{std}) of silicon.

$$D = \left(\frac{0.94}{\beta}\right) \cdot \frac{\lambda}{\cos\theta} \quad \& \quad e = \frac{\beta}{4\tan\theta} \quad \text{and} \quad \beta = \sqrt{\beta_{\text{obs}}^2 - \beta_{\text{std}}^2} \tag{1}$$

Figures 3-**??** illustrate how the microstructural parameters of the CdTe films change with varying levels of Cu doping. Specifically, it shows that the average crystallite size of the Cu-doped CdTe films increases from 16.07 nm in undoped CdTe to 28.87 nm in CdTe doped with 10 at.% Cu. This increase in crystallite size highlights the nanostructural nature of the films. As the concentration of Cu doping rises, two key observations are made: the first is the average size of the crystallites grows with higher Cu doping levels. This trend indicates that Cu2+ ions are incorporated into the CdTe lattice, which likely promotes the growth of larger crystallites. The second is a measure of the lattice distortion, decreases with increased Cu doping. This reduction suggests an improvement in the crystallinity of the CdTe films, meaning that the lattice structure becomes more ordered and defects are reduced. The successful integration of Cu2+ ions into the CdTe lattice helps in minimizing these distortions. These observations are consistent with findings reported for films doped with ions of smaller ionic radius, where doping leads to improved crystallinity and reduced microstrain [28].

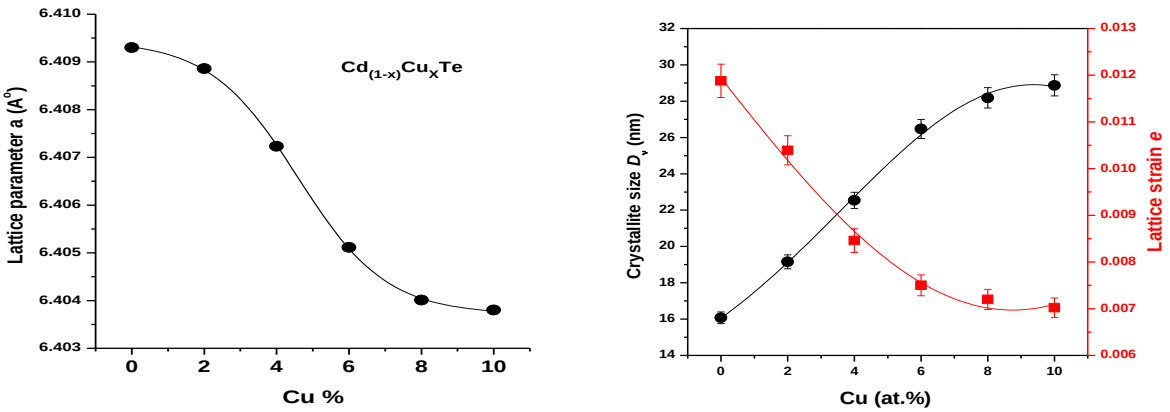

Fig. 3: (a) Structural parameters with different Cuconcentrations of undoped and Cu doped CdTe films, (b) Structural parameters with different Cu concentrations of undoped and Cu doped CdTe films..

3.2 Optical Characterization:

The optical characterization of materials offers crucial insights into their physical and electronic properties, including thickness, energy gap, and structural defects. In this study, we determined the optical band gap energy of semiconductor films by studying their absorption spectra, which were obtained through transmission and reflection measurements. Figure 4 illustrates the wavelength-dependent transmittance (T) of a nanocrystalline Cu-doped CdTe film with Cu doping levels ranging from 300 to 2500 nm. The average transmittance in the near-infrared region varied between 79% and 83%, indicating that highly transparent Cu-doped CdTe films are suitable for use as the n-type window layer in photovoltaic solar cells, comparable to the highly transmitted CdS and CdO thin films [29,30,31].

The film thickness is determined using spectroscopic ellipsometry parameters, Ψ and Δ, measured across the 300-1100 nm wavelength range. This measurement is carried out with a rotating compensator instrument, specifically the J.A. Woollam M-2000, at an incident angle of 70°. To accurately determine the film thickness, the WVASE32 program employs a detailed method involving three optical layer models, as shown in Figure 5. These models include a Cauchy

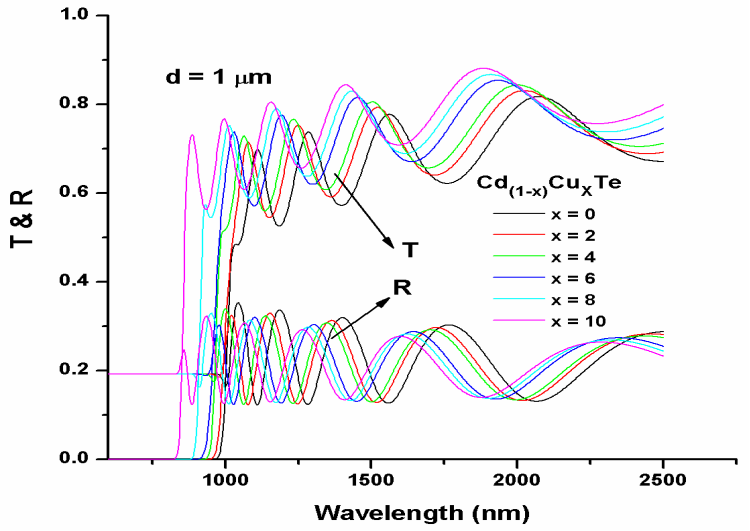

Fig. 4: The optical transmittance of Cu-free and Cu-doped CdTe films.

layer for the substrate, a B-spline layer for the Cu-doped CdTe film, and a surface roughness layer. This approach ensures precise measurement of the film thickness.

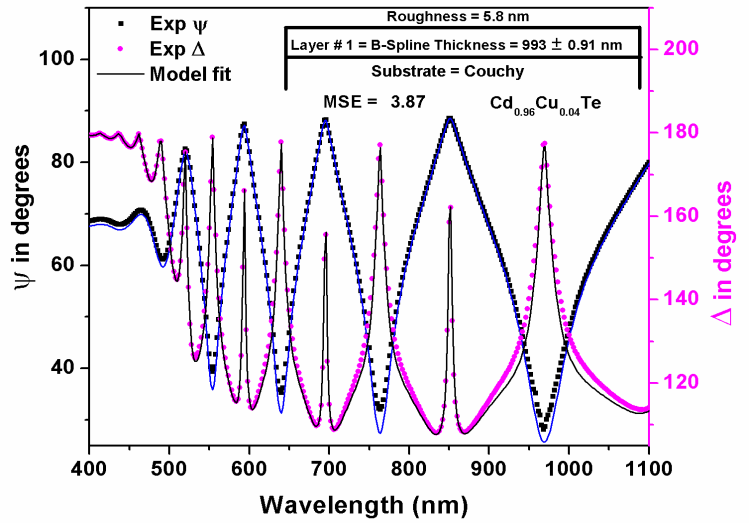

Fig. 5: Experimental and modeled ellipsometric optical parameters Ψ and Δ for calculating the film thickness Cd0.96Cu0.04Te.

The film's thickness uniformity and surface smoothness are confirmed by the appearance of interference fringes, which result from the coherent interference of multiple transmitted light waves at the film-substrate interface. Moreover, the transmission curve exhibits a sharp drop at the absorption edge, corresponding to the electron transition from the valence band (VBM) to the conduction band (CBM). As the Cu concentration in CdTe increases, the absorption edge moves to shorter wavelengths, suggesting that the fundamental energy gap of the material expands with higher Cu doping. Conversely, the transmittance rises with more Cu content, with a noticeable move in the dispersion point toward higher energy values. This behavior indicates that increasing the Cu content affects the electronic structure of the CdTe thin

film, thus enhancing the transmittance window by widening the optical band gap. To evaluate the veracity of such an expectation, the optical band gaps of the examined films were determined using their optical absorption coefficients.

$$\alpha(\lambda) = \left(\frac{1}{d}\right) \ln(X \times Y) \tag{2}$$

$$X = \left[(1-R_1)(1-R_2)(1-R_3)\right] / \left[2T(1-R_2R_3)\right] \tag{3}$$

$$Y = 1 + \left\{1 + \left[R_1(R_2 + R_3 - 2R_2R_3)\right] / (1-R_2R_3)A^2\right]\right\}^{1/2} \tag{4}$$

$$(\alpha E)^2 = B(E - E_g) \tag{5}$$

The optical absorption coefficients were determined from transmission and reflection measurements within the strong absorption region using Equations 3, 4, and 5. In these equations, d represents the film thickness, and R1, R2, and R3 denote the Fresnel reflection coefficients for the air-film interface, film-substrate interface, and substrate-air interface, respectively.

Figure 6 exhibitions the optical absorption coefficients for all tested films, while Figure 7 shows the application of Tauc's method (Eq. 6) to determine the optical band gap for direct electronic transitions in these thin films. Here α represents the optical absorption coefficient, E denotes photon energy, and B is a constant with an associated exponent [32,33,34]. The data shows that all films exhibit a high absorption coefficient (≈106 cm-1), suggesting their suitability as absorber layers in solar cells. It is evident that the absorption coefficient decreases as copper concentration increases. Additionally, there is a noticeable drop in absorption at the absorption edge, which shifts to higher energy levels with increased Cu doping.

Furthermore, the optical band gap energy rises from 1.51 eV to 1.69 eV with increasing copper doping in the CdTe lattice, a phenomenon that can be attributed to the Burstein-Moss effect. This effect occurs in degenerate semiconductors, where the Fermi level is positioned inside the conduction band. According to the Burstein-Moss effect, increased copper doping raises the electron carrier density at the conduction band edge, leading to an increased energy band gap. This is because, as doping raises the Fermi level, more electronic states are occupied below this level, making the transition from the valence band to the conduction band include higher energy. Similar observations have been reported in studies of Mo-doped CdTe films [23] and Mo-doped CdO films [35].

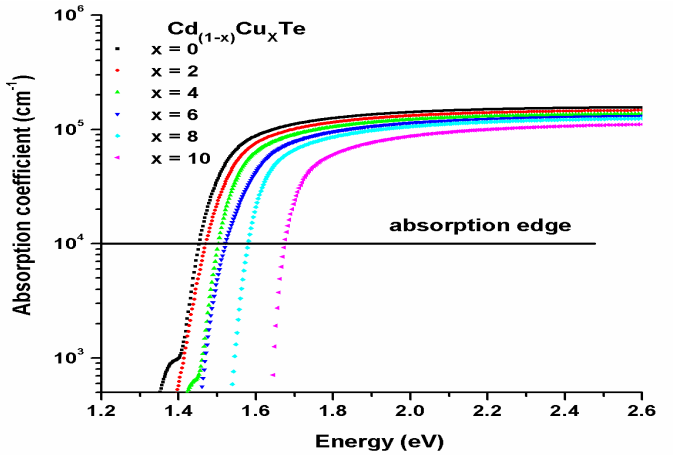

Fig. 6: The absorption coefficient versus photon energy of pure and Cu-doped CdTe films at different Cu dopants.

Optical constants such as the refractive index and extinction coefficient are crucial optoelectronic properties in the design of solar cells and photovoltaic systems. Various methods have been employed to determine the refractive index of semiconductor thin films [36,37,38,39,40,41]. For instance, the refractive index of nanostructured Cu-doped CdTe thin films was calculated using the Swanepoel method [42], which was later refined by Manifacier et al. [43]. This method involves analyzing interference patterns in transmittance spectra by constructing envelope curves around the maxima and

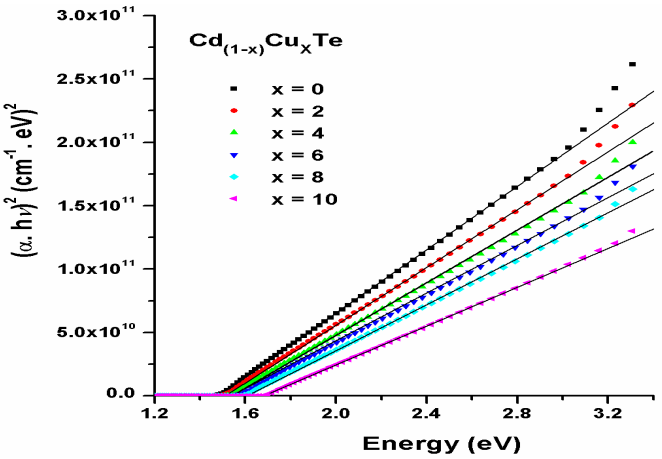

Fig. 7: $(\alpha h\nu)^2$ versus $h\nu$ of undoped and Cu-doped CdTe films at different Cu contents.

minima of transmittance. The details of this method are outlined in previous works [44,45]. Figure 8 presents the envelope for a Cu-doped CdTe thin film with 10 at.% doping, while Figure 9 shows the spectral variation of the refractive index for nanostructured Cu-doped CdTe films. This figure illustrates a typical dispersion behavior for both undoped and Cu-doped CdTe nanostructured films. It's important to recognize that as the level of Cu doping increases, the refractive index tends to decrease. This decrease is linked to the observed rise in optical band gap energy with higher Cu doping levels, a relationship that is inversely correlated according to various empirical models [46,47,48].

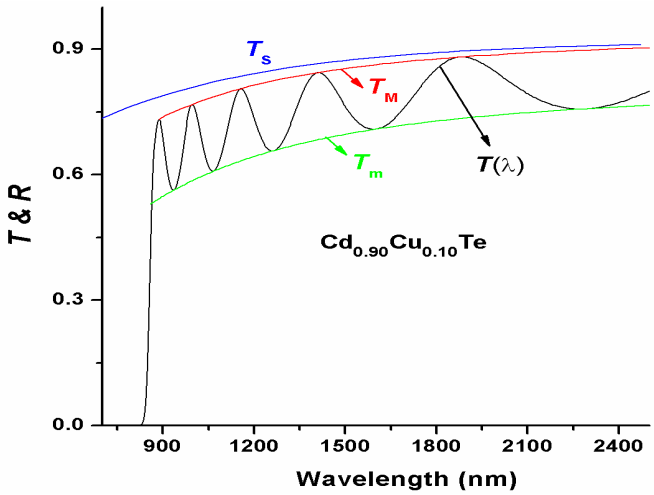

Fig. 8: The envelope of the transmittance curve of the Cu-diped CdTe (x =10 at.%) film

The Lorentz-Lorenz equation connects the refractive index directly with polarizability [49]. When Cd, with a larger atomic radius (1.61 Å), is replaced by Cu, which has a smaller atomic radius (1.45 Å), the density of the material increases, leading to reduced polarizability. Consequently, the decrease in the refractive index with higher Cu doping levels is attributed to this reduction in polarizability. Additionally, the enhancement in crystallinity and grain size of the CdTe film with increased Cu concentration could also contribute to the observed reduction in refractive index [50].

$$k = \frac{\alpha\lambda}{4\pi} \tag{6}$$

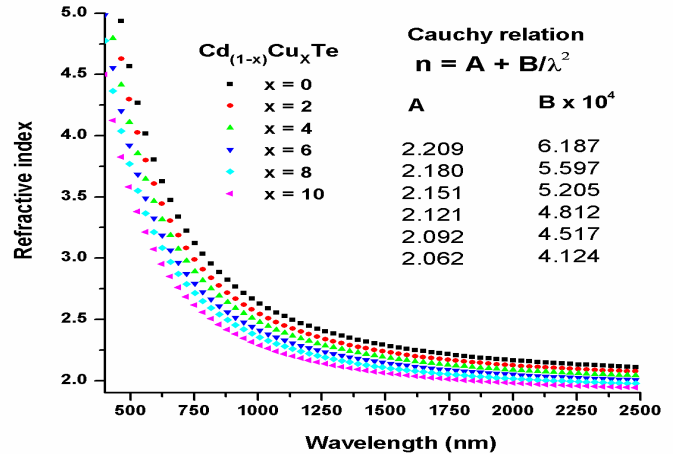

Fig. 9: The refractive of pure and Cu-doped CdTe films with different Cu concentrations.

The extinction coefficient (k) measures how much light is absorbed by a material as it passes through. For CdTe and Cu-doped CdTe films, this coefficient is calculated using a specific formula (Equation 7) [51]. Figure 10 shows how this coefficient varies with wavelength for both undoped and Cu-doped CdTe films. In regions where the material strongly absorbs light (near the fundamental absorption edge), the extinction coefficient drops sharply because most of the light is absorbed. As more Cu is added to the CdTe films, the overall extinction coefficient decreases, indicating reduced light absorption overall.

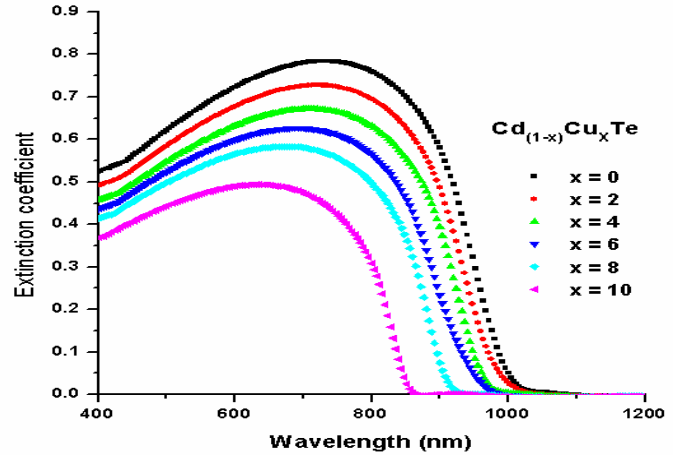

Fig. 10: The spectral variation of K for Cu doped films with various Cu doping level.

3.3 Experimental and computed absorption spectra of the examined thin films

Figure 11 shows the experimental and computed absorption α-spectra, for all tested films versus the photon energy. The computed process has been performed based on the Hydrogenic Excitonic Model (HEM) [52]. Such a model setup of a series of mathematical Eqs. (8–11) that describe the relation between the optical absorption coefficient and the photon energy in terms of the absorption strength C_0, the excitonic binding energy E_{R_0}, the line-width Γ_c of the continuum state, and Γ_m is the line-widths of the $m = 1$.

Table I contains the parameters that used to fit the experimental date. The decrease in of Co refers to an enhancement in the optical transparency of the tested films with the increase of Cu content, which is consistent with the observed

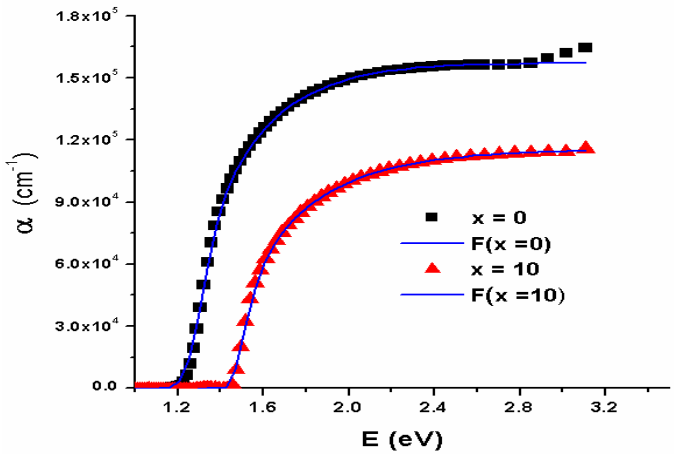

Fig. 11: The experimental and computed absorption coefficient of the films x =0 and x = 10 at.% versus photon energy.

Table 1: Optical parameters of the Hydrogenic Excitonic Model

	$x=0$ at. %	$x=2$ at. %	$x=4$ wt. %	$x=6$ at. %	$x=8$ at. %	$x=10$ at. %
$C_0, e^{1/2}$ m^{-1}	700	650	625	610	590	550
E_R, meV	1					
Γ_c, meV	10					

increased in both the optical transmittance and the optical band gap. The observed constancy in the magnitude of E_R of with the increase of Cu may revealed equivalency of the structural defects/electronic localized states. WhileThe observed in the value of the line width of the continuum Γ_c are greater than those of crystalline materials described in the literature, which could refers that the amorphous nature is the dominant in all thin films.

$$\alpha(E) = \frac{C_0 {E_R}^{1/2}}{E}\left\{\sum_{m=1}^{\infty}\frac{2E_R}{m^3}\frac{\Gamma_m}{\left(E-E_{\text{absorption edge}}\right)^2+\Gamma_m^2}+\frac{1}{2}\left[\frac{\pi}{2}+\arctan\left[\frac{E-E_{\text{direct}}}{\Gamma_c}\right]\right]-\right.$$
$$\left.\sum_{m=1}^{\infty}\frac{2E_R}{m^3}\frac{\Gamma_c}{\left(E-E_{\text{absorption edge}}\right)^2+\Gamma_c^2}+\frac{\pi}{2}\frac{\sinh\left(2u^+\right)}{\cosh\left(2u^+\right)-\cos\left(2u^-\right)}\right\} \tag{7}$$

$$u^{\pm} = \pi\left(\frac{E_R}{2}\right)^{1/2}\left[\frac{\left[\left(E-E_{\text{direct}}\right)^2+\Gamma_c^2\right]^{1/2}\pm\left(E-E_{\text{direct}}\right)}{\left(E-E_{\text{direct}}\right)^2+\Gamma_c^2}\right]^{1/2} \tag{8}$$

$$E_{\text{absorption edge}} = E_{\text{direct}} - \frac{E_R}{m^2} \tag{9}$$

$$\Gamma_m = \Gamma_c - \frac{\Gamma_c-\Gamma_1}{m^2},\ \text{m} = 1,2,3\ldots \tag{10}$$

3.4 Electric properties

Cadmium Telluride (CdTe) films doped with Copper (Cu) are of interest for applications such as high-efficiency solar cells. The electrical properties of these films, including resistivity, sheet resistance, carrier concentration, and mobility, are influenced by the amount of Cu incorporated into the CdTe matrix. The sheet resistance (R_s) thus the resistivity (*rho*) of CdTe:Cu films decrease with increasing Cu content. This decrease in resistivity indicates a higher charge carrier density. Higher charge carrier density results from an increased number of free carriers in the material, which enhances electrical conductivity. The increase in charge carriers can be attributed to the larger grain size and the presence of excess Cu cations. Larger grains reduce grain boundary scattering, which contributes to improved mobility of charge carriers. The

Table 2: Electrical parameters from Hall Effect measurement

Cu %	$R_S(\Omega)$	$\rho \times 10^{-4}$ (Ω.cm)	$\sigma \times 10^{2}(\mathrm{g.cm})^{-1}$	$R_H \times 10^{-3}$ $\left(\mathrm{cm}^3 \cdot C^{-1}\right)$	$n_H \times 10^{19}$ $\left(\mathrm{cm}^{-3}\right)$	μ_b $(\mathrm{cm}^2 \cdot V \cdot \mathrm{s}^{-1})$
0	49.9	49.9	2.005	102.1	6.12	20.48
2	13.6	13.6	7.366	79.92	7.82	58.88
4	6.68	6.68	14.98	61.79	10.12	92.57
6	3.08	3.08	32.52	33.58	18.62	109.2
8	1.95	1.95	51.28	24.19	25.84	124
10	1.65	1.65	60.61	21.75	28.73	131.8

sheet resistance (R_s) and resistivety (ρ) measurements are a measure of the resistance of a film to current flow, normalized by the thickness of the film. The formula (R_s) and (ρ) in a four-point probe measurement is given by Eqs. 12 and 13 [53], where (V) is the voltage applied across the film, (I) is the current passing through it, the value 4.53 is a correction factor to account for the specific geometry of the probe and d is the film thickness.

$$R_{\mathrm{s}} = 4.53 \frac{\mathrm{V}}{\mathrm{I}} [\Omega/\mathrm{sq}] \tag{11}$$

$$\rho = R_{\mathrm{s}} d \tag{12}$$

The relationship between the sheet resistance of the CdTe:Cu films and the Cu content is shown in Figure 12 (a). It can be seen from that, the value of Rs decreases significantly with increasing Cu content. For instance, as the Cu content increases from 0 at.% to 10 at.%, R_s decreases from 49.9 Ω to 1.65 Ω. This reduction demonstrates improved electrical conductivity with higher Cu doping. Also, Hall Effect measurements provide information on the type of charge carriers (in our case, p-type), carrier concentration (nH), and Hall mobility (μb).The films are confirmed to be p-type semiconductors, which means that the dominant charge carriers are holes. The results show that as the Cu content increases, the carrier concentration also increases. This is expected as more Cu introduces more free holes into the CdTe matrix. The Hall mobility increases with Cu content. Typically, an increase in mobility is associated with a reduction in grain boundary scattering, which is a consequence of increased crystallite size. As the grain size increases, fewer scattering centers are present, allowing charge carriers to move more freely. The increasing in carriers concentration and the Hall mobility against Cu content are shown in Figure 12 (b). Table 2. displays all Hall measurements for CdTe:Cu films as a function of Cu concentration.

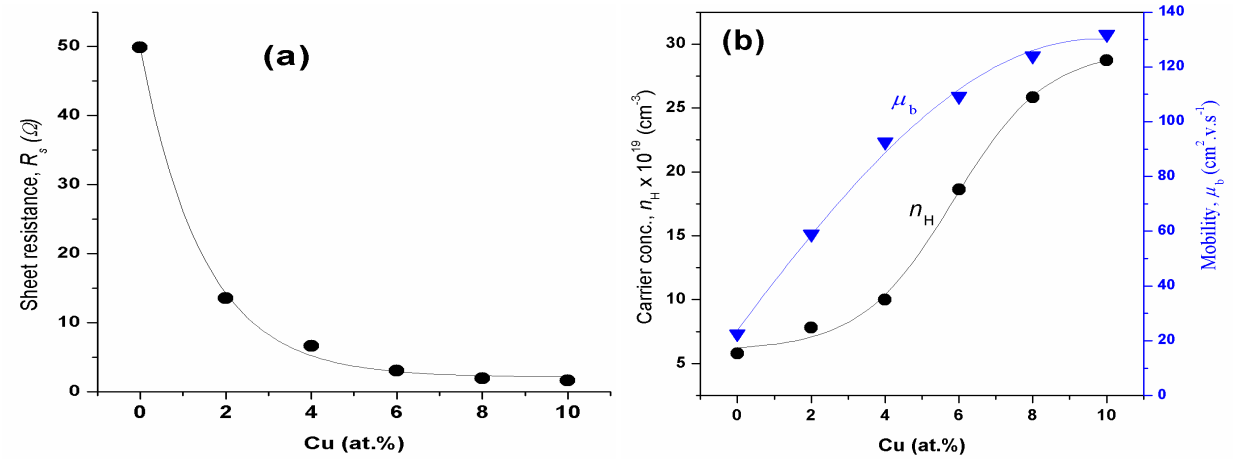

Fig. 12: (a) Sheet resistance, Rs and (b) Carrier concentration, nH and Mobility, μb as a function of Cu content for CdTe:Cu films.

4 Conclusions

In this study, Cu-doped CdTe ingots with copper concentrations ranging from 0 to 10% by weight were produced using a mechanical ball milling process. These ingots were then shaped into disks and utilized as sources for thin film deposition through electron beam evaporation at room temperature. Structural analysis via X-ray diffraction (XRD) and energy-dispersive X-ray spectroscopy (EDXS) confirmed the successful incorporation of Cu into the CdTe matrix while preserving its cubic structure. Optical evaluations revealed that higher Cu concentrations led to larger crystallite sizes and reduced microstrain, thereby enhancing the material's crystallinity. Additionally, the absorption edge exhibited a blueshift, indicating an increase in the optical band gap. Higher Cu doping levels also resulted in a lower refractive index and a significant reduction in the extinction coefficient in the strong absorption region. These results suggest that Cu-doped CdTe films, with their improved transparency and optimized band gap, are promising for photovoltaic solar cell applications. A comparison of experimental and theoretical absorption spectra using the Hydrogenic Excitonic Model (HEM) shows that increasing Cu concentration enhances optical transparency and band gap. The observed uniformity of structural flaws and broader line widths, compared to crystalline materials, indicate that the films are predominantly amorphous. Hall measurements reveal that the CdTe:Cu films are p-type, with sheet resistance (R_s) decreasing from 49.9 Ω to 1.65 Ω as Cu content increases from 0 to 10%. The carrier concentration (nH) and Hall mobility (μb) of the CdTe:Cu films increase with higher Cu levels, with improved mobility attributed to reduced grain boundary scattering as crystallite size grows.

Conflict of Interest

I declare that there is no conflict of interest regarding the publication of this paper.

Acknowledgement

The authors are thankful to the Deanship of Scientific Research at University of Bisha for supporting this work through the Fast-Track Research Support Program.

References

[1] Y. Chen, X. Zhang and Q. Wu, Cadmium telluride thin film solar cells: A review of advances in fabrication and performance, *Materials Science and Engineering: R: Reports* **135** (2019) 22–50.
[2] J. Pereira, I. Pacheco and C. Alves, Impact of copper doping on the optical properties of cdte thin films., *Journal of Applied Physics* **128**(12) (2020) p. 125305.
[3] S. T. Sundari, A. K. T. V. Swaminathan and T. Mahalingam, "microstructural studies of oxygen irradiated cdte thin films, *Physica Status Solidi (A)* **177**(2) (2000) 495–502.
[4] C. Polop, I. Mora-Sero, C. Munuera, J. G. de Andres, V. Munoz-Sanjose and C. Ocal, Twin coarsening in cdte (1 1 1) films grown on gaas (1 0 0), *Acta materialia* **54**(16) (2006) 4285–4291.
[5] M. Niraula, K. Yasuda, T. Ishiguro, Y. Kawauchi, H. Morishita and Y. Agata, Metal-organic vapor-phase epitaxy growth and characterization of thick (100) cdte layers on (100) gaas and (100) gaas/si substrates, *Journal of electronic materials* **32** (2003) 728–732.
[6] N. Lovergine, P. Prete, L. Tapfer, F. Marzo and A. M. Mancini, Hydrogen transport vapour growth and properties of thick cdte epilayers for rt x-ray detector applications, *Crystal Research and Technology: Journal of Experimental and Industrial Crystallography* **40**(10-11) (2005) 1018–1022.
[7] P. Banerjee, R. Ganguly and B. Ghosh, Optical properties of cd1- xznxte thin films fabricated through sputtering of compound semiconductors, *Applied surface science* **256**(1) (2009) 213–216.
[8] K. Garadkar, S. Pawar, P. Hankare and A. Patil, Effect of annealing on chemically deposited polycrystalline cdte thin films, *Journal of alloys and Compounds* **491**(1-2) (2010) 77–80.
[9] F. de Moure-Flores, J. Quiñones-Galván, A. Guillén-Cervantes, J. Arias-Cerón, A. Hernández-Hernández, J. Santoyo-Salazar, J. Santos-Cruz, S. Mayén-Hernández, M. d. l. L. Olvera, J. Mendoza-Álvarez *et al.*, Cdte thin films grown by pulsed laser deposition using powder as target: Effect of substrate temperature, *Journal of crystal growth* **386** (2014) 27–31.
[10] V. Kosyak, A. Opanasyuk, P. Bukivskij and Y. P. Gnatenko, Study of the structural and photoluminescence properties of cdte polycrystalline films deposited by close-spaced vacuum sublimation, *Journal of Crystal Growth* **312**(10) (2010) 1726–1730.
[11] R. R. Singh, D. Painuly and R. Pandey, Synthesis and characterization of electrochemically deposited nanocrystalline cdte thin films, *Materials Chemistry and Physics* **116**(1) (2009) 261–268.

[12] E. R. Shaaban, N. Afify and A. El-Taher, Effect of film thickness on microstructure parameters and optical constants of cdte thin films, *Journal of Alloys and Compounds* **482**(1-2) (2009) 400–404.
[13] K. Punitha, R. Sivakumar, C. Sanjeeviraja, V. Sathe and V. Ganesan, Physical properties of electron beam evaporated cdte and cdte: Cu thin films, *Journal of Applied Physics* **116**(21) (2014).
[14] C. Doroody, K. Rahman, S. Abdullah, M. Harif, H. Rosly, S. Tiong and N. Amin, Temperature difference in close-spaced sublimation (css) growth of cdte thin film on ultra-thin glass substrate, *Results in Physics* **18** (2020) p. 103213.
[15] M. Islam, H. Misran, M. Akhtaruzzaman, N. Amin *et al.*, Influence of oxygen on structural and optoelectronic properties of cds thin film deposited by magnetron sputtering technique, *Chinese Journal of Physics* **67** (2020) 170–179.
[16] Z. Xie, Y. Sui, J. Buckeridge, C. R. A. Catlow, T. W. Keal, P. Sherwood, A. Walsh, M. R. Farrow, D. O. Scanlon, S. M. Woodley *et al.*, Donor and acceptor characteristics of native point defects in gan, *Journal of Physics D: Applied Physics* **52**(33) (2019) p. 335104.
[17] B. Choudhury, M. Dey and A. Choudhury, Shallow and deep trap emission and luminescence quenching of tio 2 nanoparticles on cu doping, *Applied Nanoscience* **4** (2014) 499–506.
[18] S. Patel, A. Thakur, M. Kannan, M. Dhaka *et al.*, Analysis of different annealing conditions on physical properties of bi doped cdte thin films for potential absorber layer in solar cells, *Solar Energy* **199** (2020) 772–781.
[19] A. Kumar, R. Singh and S. Sharma, Structural characterization of copper-doped cdte thin films: A comprehensive study, *Journal of Materials Science: Materials in Electronics* **32**(6).
[20] R. Singh, A. Kumar and P. Rani, Effect of copper doping on the crystalline properties of cdte thin films, *Thin Solid Films* **734** (2022) p. 138957.
[21] K. A. Aris, K. S. Rahman, A. M. Ali, B. Bais, I. B. Yahya, M. Akhtaruzzaman, H. Misran, S. F. Abdullah, M. A. Alghoul and N. Amin, A comparative study on thermally and laser annealed copper and silver doped cdte thin film solar cells, *Solar Energy* **173** (2018) 1–6.
[22] K. Reddy, P. Kumar and P. Agarwal, Optical properties of cu-doped cdte films: Bandgap modifications and photoluminescence., *Advanced energy materials* **31**(7) (2023) 1080–1093.
[23] X. Jiang, H. Zhang and L. Zhao, Electrical properties and carrier dynamics of cu-doped cdte thin films., *IEEE Transactions on Electron Devices* **71**(3) (2024) 1200–1206.
[24] T. Manimozhi, T. Logu, J. Archana, M. Navaneethan, K. Sethuraman and K. Ramamurthi, Enhanced photo-response of cdte thin film via mo doping prepared using electron beam evaporation technique, *Journal of Materials Science: Materials in Electronics* **31** (2020) 21059–21072.
[25] M. El-Hagary, S. H. Moustafa, H. Hashem, E. R. Shaaban and M. Emam-Ismail, Influences of mn doping on the microstructural, semiconducting, and optoelectronic properties of hgo nanostructure films, *Journal of the American Ceramic Society* **102**(8) (2019) 4737–4747.
[26] M.-H. Cho, D.-H. Ko, K. Jeong, S. Whangbo, C. Whang, S. Choi and S. Cho, Growth stage of crystalline y 2 o 3 film on si (100) grown by an ionized cluster beam deposition, *Journal of Applied Physics* **85**(5) (1999) 2909–2914.
[27] M. Thangaraju, A. Jayaram and R. Kandasamy, Structural, morphological, optical and electrical properties of e-beam deposited nanocrystalline cdte: Cu alloy thin films from mechanical alloyed samples, *Applied Surface Science* **449** (2018) 2–9.
[28] M. Dehimi, T. Touam, A. Chelouche, F. Boudjouan, D. Djouadi, J. Solard, A. Fischer, A. Boudrioua and A. Doghmane, Effects of low ag doping on physical and optical waveguide properties of highly oriented sol-gel zno thin films, *Advances in Condensed Matter Physics* **2015**(1) (2015) p. 740208.
[29] L. Ma, X. Ai and X. Wu, Effect of substrate and zn doping on the structural, optical and electrical properties of cds thin films prepared by cbd method, *Journal of alloys and compounds* **691** (2017) 399–406.
[30] J. Zhou, X. Wu, G. Teeter, B. To, Y. Yan, R. Dhere and T. Gessert, Cbd-cd1- xznxs thin films and their application in cdte solar cells, *physica status solidi (b)* **241**(3) (2004) 775–778.
[31] N. Makori, I. Amatalo, P. Karimi and W. Njoroge, Optical and electrical properties of cdo: Sn thin films for solar cell applications, *Int. J. Optoelectron. Eng* **4**(1) (2014) 11–15.
[32] J. Tauc, *In: Optical properties of Solids Abeles F* (editor Amsterdam North-Holland, 1969).
[33] E. Davis and N. Mott, Conduction in non-crystalline systems v. conductivity, optical absorption and photoconductivity in amorphous semiconductors, *Philosophical magazine* **22**(179) (1970) 0903–0922.
[34] B. D. Viezbicke, S. Patel, B. E. Davis and D. P. Birnie III, Evaluation of the tauc method for optical absorption edge determination: Zno thin films as a model system, *physica status solidi (b)* **252**(8) (2015) 1700–1710.
[35] R. Kumaravel, S. Bhuvaneswari, K. Ramamurthi and V. Krishnakumar, Structural, optical and electrical properties of molybdenum-doped cadmium oxide thin films prepared by spray pyrolysis method, *Applied Physics A* **109** (2012) 579–584.
[36] G. Jellison Jr and F. Modine, Parameterization of the optical functions of amorphous materials in the interband region, *Applied Physics Letters* **69**(3) (1996) 371–373.
[37] S. Jena, R. Tokas, S. Thakur and D. Udupa, Study of aging effects on optical properties and residual stress of hfo2 thin film, *Optik* **185** (2019) 71–81.
[38] D. Minkov, Calculation of the optical constants of a thin layer upon a transparent substrate from the reflection spectrum, *Journal of Physics D: Applied Physics* **22**(8) (1989) p. 1157.
[39] J. Gonzalez-Leal, E. Marquez, A. Bernal-Oliva, J. Ruiz-Perez and R. Jimenez-Garay, Derivation of the optical constants of thermally-evaporated uniform films of binary chalcogenide glasses using only their reflection spectra, *Thin Solid Films* **317**(1-2) (1998) 223–227.

[40] M. Emam-Ismail, M. El-Hagary, E. Shaaban and S. Althoyaib, Structural and optical investigation of nanocrystalline zn1- xnixs diluted magnetic semiconductor thin films, *Journal of alloys and compounds* **529** (2012) 113–121.
[41] M. Emam-Ismail, E. Shaaban and M. El-Hagary, A new method for calculating the refractive index of semiconductor thin films retrieved from their transmission spectra, *Journal of Alloys and Compounds* **663** (2016) 20–29.
[42] R. Swanepoel, Determination of the thickness and optical constants of amorphous silicon, *Journal of Physics E: Scientific Instruments* **16**(12) (1983) p. 1214.
[43] J. Manifacier, J. Gasiot and J. Fillard, A simple method for the determination of the optical constants n, k and the thickness of a weakly absorbing thin film, *Journal of Physics E: Scientific Instruments* **9**(11) (1976) p. 1002.
[44] M. El-Hagary, M. Emam-Ismail, E. Shaaban and I. Shaltout, Optical properties of glasses (teo2–geo2–k2o) thin films co-doped with rare earth oxides sm2o3/yb2o3, *Journal of alloys and compounds* **485**(1-2) (2009) 519–523.
[45] E. Shaaban, M. El-Hagary, M. Emam-Ismail and M. El-Den, Optical band gap, refractive index dispersion and single-oscillator parameters of amorphous se70s30- xsbx semiconductor thin films, *Philosophical Magazine* **91**(12) (2011) 1679–1692.
[46] T. Moss, A relationship between the refractive index and the infra-red threshold of sensitivity for photoconductors, *Proceedings of the Physical Society. Section B* **63**(3) (1950) p. 167.
[47] N. Ravindra, S. Auluck and V. Srivastava, On the penn gap in semiconductors, *Physica status solidi (b)* **93**(2) (1979) K155–K160.
[48] P. Herve and L. Vandamme, Empirical temperature dependence of the refractive index of semiconductors, *Journal of Applied Physics* **77**(10) (1995) 5476–5477.
[49] S. Elliott, *The physics and chemistry of solids* (John Wiley & Sons, 1998).
[50] K. Senthil, D. Mangalaraj, S. K. Narayandass and S. Adachi, Optical constants of vacuum-evaporated cadmium sulphide thin films measured by spectroscopic ellipsometry, *Materials Science and Engineering: B* **78**(1) (2000) 53–58.
[51] E. Shaaban, M. El-Hagary, M. Emam-Ismail, A. Abd Elnaeim, S. Moustafa and A. Adel, Optical characterization of polycrystalline znse1- xtex thin films using variable angle spectroscopic ellipsometry and spectrophotmetery techniques, *Materials Science in Semiconductor Processing* **39** (2015) 735–741.
[52] J. Peng and J. Wu, A numerical simulation model of the induce polarization: Ideal electric field coupling system for underwater active electrolocation method, *IEEE Transactions on Applied Superconductivity* **26**(7) (2016) 1–5.
[53] R. C. Jaeger, *Introduction to microelectronic fabrication* (Addison-Wesley Longman Publishing Co., Inc., 1987).